XLVI CILAMCE
VITÓRIA - ES - BRAZIL - 2025
XLVI IBERO-LATIN AMERICAN CONGRESS ON COMPUTATIONAL METHODS IN ENGENEERING

Biomechanical Modeling of Gluteus Maximus Contribution to Pedal Torque

Wentz, A. Viegas[1], De Leon, Daniel M.[1]

[1]*Dept. of Mechanical Engineering, Federal University of Rio Grande do Sul*
Sarmento Leite, 425, 90050-170, RS, Brazil
wentz.andre@gmail.com, daniel.leon@ufrgs.br

Abstract. This work presents a biomechanical model of a cyclist in the sagittal plane, simulating the motion of the leg and pedal based on a four-bar linkage mechanism. Inverse kinematics is used to determine the positions of the lower limb segments throughout the pedaling cycle, and the force calculations are performed using inverse dynamics. A system of linear equations is formulated to compute joint reaction forces and the crank torque from joint moments. The Gluteus Maximus muscle is modeled using real anatomical data such as physiological cross-sectional area (PCSA), specific muscle tension, muscle activation, and the behavior of the muscle's moment arm over the femoral head. Muscle force is estimated using a Hill-type model, where muscle elongation is considered in order to represent the nonlinear behavior of the muscle–tendon unit. The resulting analysis allows the evaluation of the torque generated by the Gluteus Maximus during the pedaling cycle, enabling the identification of optimal activation positions and the instants where the activation will produce isometric contractions that do not contribute to the generation of crank torque. This analysis is especially important when designing the bicycle frame and its drivetrain to ensure efficient load transfer throughout the pedaling motion.

Keywords: Cycling Biomechanics, Muscle Force Modeling, Gluteus Maximus Activation

1 Introduction

The efficiency of power transmission is an important topic in engineering and biomechanics research of bicycle components. One way to increase this efficiency is to improve the cyclist's force application on the bicycle drivetrain. Among the proposed solutions, the use of non-circular chainrings stands out, as it allows for a variation of the gear ratio throughout the pedaling cycle, better adapted to the variable muscular abilities of the cyclist. However, determining the optimal shape for such a chainring remains a significant technical and scientific challenge.

According to Juhl [1], a properly optimized noncircular chainring can enhance cycling performance by allowing the muscles to more efficiently generate tangential forces on the pedals through a more favorable crank angular velocity profile, resulting from the variable gear ratio. Furthermore, this geometry can reduce the time spent in low-torque phases and increase the time in high-torque phases, improve mechanical power transmission by altering the chain's lever arm throughout the crank revolution, and enhance the contribution of inertial forces to power output. However, these benefits can only be achieved when the shape of the chainring is carefully adapted to the muscular capacities and the dynamic behavior of the human body during pedaling.

The challenge of designing these components arises mainly from the complexity of modeling the interaction between the musculoskeletal system and the bicycle drivetrain. The torque applied to the crank is not only a function of the geometry of the bicycle or joint motion, but also of the internal dynamics of the leg, the non-linear behavior of muscle-generated forces throughout the pedaling cycle and the coordination among muscle groups. As highlighted by Redfield and Hull [2], the lower limb system is indeterminate with respect to muscle forces, since more muscles act on each joint than there are degrees of freedom on the leg. This requires the use of constrained optimization procedures or the grouping of muscles into functional units in order to create a deterministic and solvable system.

Moreover, mechanical demands during cycling are not constant. During uphill cycling, riders must overcome gravity, which significantly increases mechanical power demands. Due to the slope of the surface, cyclists must adapt their posture for two main reasons: first, to avoid lifting the front wheel off the ground and second, to maintain a stable seated position and prevent sliding. Mountain bikers face even more challenging terrain conditions, requiring sufficient rear wheel traction while ensuring that the front wheel remains in contact with the ground. To

achieve this, they lean their trunks and shift their bodies forward in the saddle. This postural adjustment alters several characteristics of pedaling, potentially leading to changes in mechanical demands, energy economy, power efficiency, pedal kinematics and neuromuscular activation patterns (Fonda and Šarabon [3]). This is why a realistic parametric musculoskeletal model is essential for optimizing a non-circular chainring, rather than relying solely on a fixed force profile measured from a live cyclist.

In this work, a two-dimensional biomechanical model is developed based on a four-bar linkage mechanism that represents the cyclist's leg motion in the sagittal plane. From the joint positions obtained through inverse kinematics, the torque applied to the crank is calculated while accounting for the nonlinear characteristics of muscle activation and articular join distances.

2 Biomechanical Model

2.1 Four link leg model

To represent the motion of the cyclist's lower limb during pedaling, a planar multibody model was implemented as an closed kinematic chain. This approach is commonly used in biomechanical analyses due to its ability to capture the segmental behavior of the leg while maintaining computational efficiency. The model consists of rigid segments representing the thigh, shank, foot, and crank arm, interconnected at the hip, knee, ankle, and pedal joints. The positions of these joints are determined using geometric and trigonometric relationships based on the known lengths of each segment and the joint angles throughout the crank cycle. By assuming motion confined to the sagittal plane, the model simplifies the three-dimensional complexity of pedaling while still capturing the essential kinematic characteristics relevant to torque production and force transmission. This formulation provides the necessary joint positions and segment orientations to subsequently compute muscle lever arms, joint torques, and, ultimately the resultant forces applied to the pedal. In Figure 1, we can see the linkage model and the biker leg dimensions according to Table 1. Those dimensions were taken from the author's own leg, but the software can be tuned for anyone, just by measuring the subject main articulation distances and body mass.

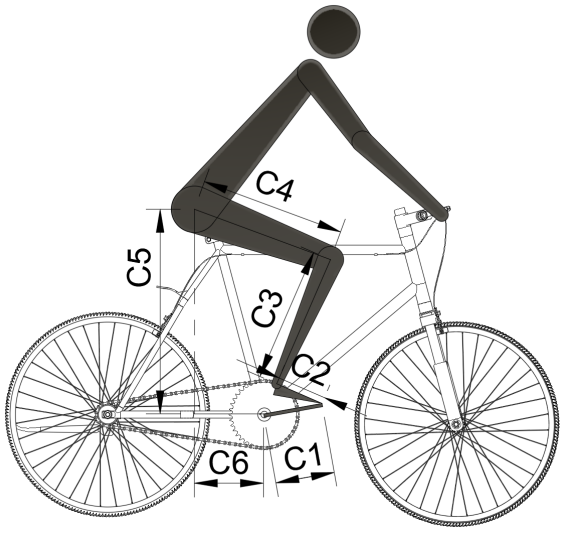


Figure 1. Linkage model and bikers dimensions

Looking at the mechanism, we can count up to 5 links, since the theory states that there is a link between the hip joint and the crankcase. To solve for this, some researches like Hull and Jorge [4] try to guess the ankle movement, imposing a sine function on the ankle angle, ranging from approximately -20° to 20°, in phase with the pedaling cycle. With the purpose of simplify the problem, and remembering that the model will be use to find a non-circular chainring, here the angle between the shank and the foot is fixed at 90°, making it a four bar mechanism.

Table 1. Biker dimensions

Description	Nomenclature	Value [mm]
Crank	$C1$	180
Foot	$C2$	150
Tibia	$C3$	410
Femur	$C4$	440
Seat vertical distance	$C5$	620
Seat horizontal distance	$C6$	210

2.2 Static Equilibrium Model

Using the joint angles and positions, we are able to compute forces and moments on the linkage connections. A classic approach to solving this problem is to create a linear system of equations of type $Ax = b$ and solve it for all angles in a pedaling cycle. An advantage of this strategy, from the biomechanical point of view, is that we can work with internal (muscle) and external (pedal reaction) forces at the same time. In eq. (1), we can see the complete system of equations, corresponding to the variables shown in Fig. 2 .

$$\begin{bmatrix} 1 & 0 & 1 & 0 & 0 & 0 & 0 & 0 & 0 & 0 & 0 & 0 \\ 0 & 1 & 0 & 1 & 0 & 0 & 0 & 0 & 0 & 0 & 0 & 0 \\ -\mathrm{r_{thy}} & \mathrm{r_{thx}} & \mathrm{r_{tky}} & -\mathrm{r_{tkx}} & 0 & 0 & 0 & 0 & 0 & 0 & 0 & 0 \\ 0 & 0 & 1 & 0 & 1 & 0 & 0 & 0 & 0 & 0 & 0 & 0 \\ 0 & 0 & 0 & 1 & 0 & 1 & 0 & 0 & 0 & 0 & 0 & 0 \\ 0 & 0 & -\mathrm{r_{sky}} & \mathrm{r_{skx}} & \mathrm{r_{say}} & -\mathrm{r_{sax}} & 0 & 0 & 0 & 0 & 1 & 0 \\ 0 & 0 & 0 & 0 & 1 & 0 & 1 & 0 & 0 & 0 & 0 & 0 \\ 0 & 0 & 0 & 0 & 0 & 1 & 0 & 1 & 0 & 0 & 0 & 0 \\ 0 & 0 & 0 & 0 & -\mathrm{r_{fay}} & \mathrm{r_{fax}} & \mathrm{r_{fpy}} & -\mathrm{r_{fpx}} & 0 & 0 & 1 & 0 \\ 0 & 0 & 0 & 0 & 0 & 0 & 1 & 0 & 1 & 0 & 0 & 0 \\ 0 & 0 & 0 & 0 & 0 & 0 & 0 & 1 & 0 & 1 & 0 & 0 \\ 0 & 0 & 0 & 0 & 0 & 0 & -\mathrm{r_{lpy}} & \mathrm{r_{lpx}} & \mathrm{r_{lcy}} & -\mathrm{r_{lcx}} & 0 & 1 \end{bmatrix} \begin{bmatrix} F_{hx} \\ F_{hy} \\ F_{kx} \\ F_{ky} \\ F_{ax} \\ F_{ay} \\ F_{px} \\ F_{py} \\ F_{sx} \\ F_{sy} \\ M_{\mathrm{Ankle}} \\ M_{\mathrm{Crank}} \end{bmatrix} = \begin{bmatrix} 0 \\ m_{\mathrm{Th}}.g \\ M_{Hp} + M_{kn} \\ 0 \\ m_{\mathrm{Sh}}.g \\ M_{Kn} \\ 0 \\ m_{\mathrm{Ak}}.g \\ 0 \\ 0 \\ m_{\mathrm{Cr}}.g \\ 0 \end{bmatrix} \tag{1}$$

In vector b from eq. (1), we have the moment created by the upper leg muscles around the femur head attachment on the hip M_{Hp} and the moment around the knee created by the lower leg muscles, M_{Kn}. All of these are input variables, but for this study, only the torque created by the gluteus maximus around the head of the femur will be included. As a consequence, in the x vector, we will find as unknowns all the forces on the joints, the moment around the knee M_{Ankle} and the moment around the crankcase M_{Crank}. The first, M_{Ankle}, will result in the effort required to respect the condition stated in section 2.1, where the angle between the foot and the shank should always be 90°. The second, M_{Crank}, is the result we are looking for, that is, the actual torque applied to the bicycle transmission system.

The distances from the center of mass of all body members were obtained from the article from Chandler et al. [5], where anthropometric measurements were made of six male cadavers, providing an average center of gravity location and moments of inertia of those body parts. The values used in the calculations can be seen in Table 2.

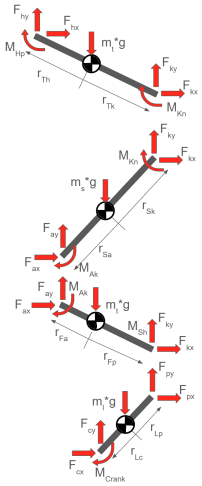


Figure 2. Free body diagram and center of mass of the thigh, shank, foot and bicycle crank.

Table 2. CG center proximal/length ratio.

Segment	Length Index	Ratio
Thigh	$C4$	0.398
Shank	$C3$	0.413
Foot	$C2$	0.4
Crank	$C1$	0.5

2.3 Muscle force model

The muscle force model is based on classical biomechanical principles, combining anatomical and physiological properties to estimate the force generated by the gluteus maximus during pedaling. Active force is calculated from physiological cross-sectional area (PCSA), specific muscle tension (σ), degree of muscle activation, force-velocity factor (fv) and pennation angle composing an approach based on the Hill-type model. Additionally, the program incorporates a force–length relationship modeled by a Gaussian function, which adjusts muscle force according to the joint angle, reflecting the physiological variation in force generation capacity throughout the pedal cycle. The muscle moment arm is determined by a polynomial dependent on the angle, allowing the torque generated by the gluteus to be calculated dynamically and realistically for each pedal position, integrating anatomical and functional factors in a detailed analysis of muscle force production. The complete equation for the active force produced by the gluteus maximus, as a function of muscle length l, contraction velocity v, and time t, is presented in eq. (2). In this expression, Act(t) represents the level of neural activation, PCSA_{Gl} is the physiological cross-sectional area of the muscle, σ denotes the specific muscle tension, f_l is the force–length scaling factor, f_v is the force–velocity scaling factor, and θ_{pen} is the muscle pennation angle.

$$F_{\text{Gl}}(l, v, t) = \text{Act(t)} \cdot \text{PCSA}_{\text{Gl}} \cdot \sigma \cdot f_l(l) \cdot f_v(v) \cdot \cos(\theta_{\text{pen}}) \tag{2}$$

In this study, since we are focus on a quasi-static state, a few simplifications are made. Neuronal activation and the force-velocity scaling factor are set to one, which means that the muscle is generating all possible tension force, and the second is needed to prevent a reduction in muscle force that occurs from high-speed movements. In doing this, the total muscular force is only dependent on the muscle length (l), a variable that can be related to our four-bar linkage model. The remaining constants are PCSA_{Gl}, θ_{pen} and σ were obtained from the literature. The physiological cross section area of the muscle and the pennation angles were used from Ward et al. [6], and are $33.4\ \text{cm}^2$ and $21.9°$, respectively. The specific muscle tension was chosen as $26.8\ \text{N/cm}^2$ according to Persad et al. [7] .

An important non-linear aspect of muscle force is its behavior in relation to muscle elongation. There is a sweet spot on the muscle length, where it can develop the maximum sarcomere overlap, before passive forces start to reduce the net force on the tendons. To reproduce this phenomenon, a simplified Hill model was developed

using a Gaussian-shaped function like the work of Thelen [8]. In this equation, L is the muscle length in the resting position and w is a shape factor chosen to be 0.45 according to the article.

$$f_L(L) = \exp\left(-\left(\frac{L - L_0}{w}\right)^2\right) \tag{3}$$

Since the gluteus maximus reaches its maximum force-generating capacity when the hip is in a neutral or slightly extended position, typically around 0° to 15° of hip extension, the available muscle force increases during the pedal cycle. This happens because the muscle is activated in a very elongated state and ends the contraction before reaching the neutral/relaxed position. The typical force vs. length relation can be seen in Fig. 3, where the relaxed and elongated positions of the muscle are shown over the curve. That curve is an approximation, inspired by the work of Murray et al. [9] that did this representation on the muscles around the elbow. Unfortunately, it was not possible to find an anatomical measurement of the sarcomere length for gluteus maximus in relation to the position of the leg, but the assumptions made in the Fig. 3, correlate well with the findings made about cyclists in the work of Rassier et al. [10].

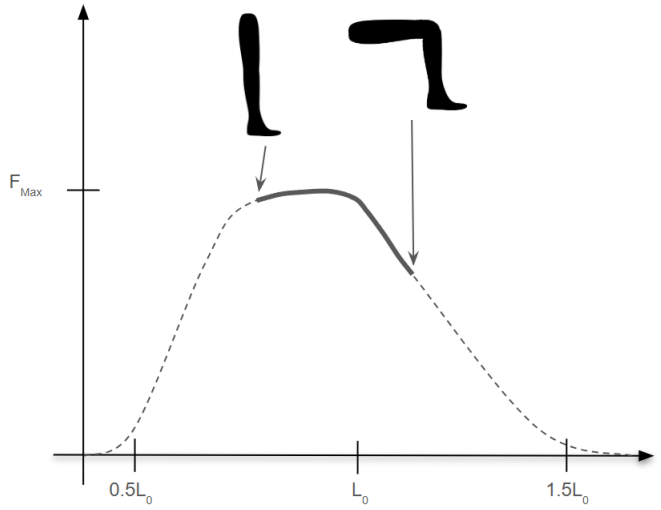


Figure 3. Typical Gluteus Maximus force-length relationship. The figure shows a reduction in available force with respect to the thigh flexion angle.

2.4 Articular moment arm

To obtain the moment generated on the hip joint, M_{Hp} in Fig. 2, one can simply multiply the muscle force F_{Gl} by the distance from the head of the femur. However, this distance is not constant, and a number of articles show different techniques for measuring it [6, 11–15]. In Fig. 4 we see the curve recreated from Németh and Ohlsén [14], this reference was chosen because it has the longest arc range of the moment arm measure, showing how the moment arm reduces significantly during a thigh flex. This is important because the cyclist seated position places the leg in a condition where this important muscle is not utilized in its optimal form.

The calculation of the muscle moment arm for the gluteus maximus in this study was based on a polynomial function that relates the moment arm length to the hip joint angle and extrapolating its values after $90°$. Specifically, the moment arm is modeled as a fifth-degree polynomial of the hip angle, with coefficients fitted to experimental data seen in Fig. 4. This approach allows the moment arm to vary dynamically as the hip moves through its range of motion, reflecting the anatomical reality that the effectiveness of muscle force transmission changes with joint position. By evaluating this polynomial for each pedal cycle position, we obtain a realistic estimate of the gluteus maximus moment arm at every angle. This value is then multiplied by the muscle force to calculate the moment generated at the hip, ensuring that both anatomical and functional variability are incorporated into the biomechanical analysis. This method provides a more physiologically accurate representation of muscle mechanics

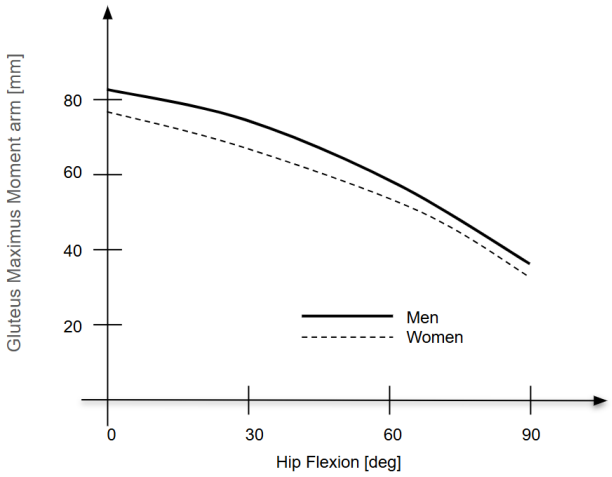


Figure 4. Mean moment arm length for Gluteus Maximus, adapted from Németh and Ohlsén [14].

compared to using a constant moment arm and is particularly important for future optimization goals using the modeling of cycling forces.

3 Results and Discussion

Compiling the contribution of all the models, we can calculate a graphic view of the cyclist's lower limb in a 360° rotation around the crankshaft. The program, made using Python language, shows that it is possible to obtain a parametric model that is very useful to be used in an optimization algorithm. This allow the calculation of new bike frames or drivetrain configurations to better produce torque using the user's anatomy as an input to the design.

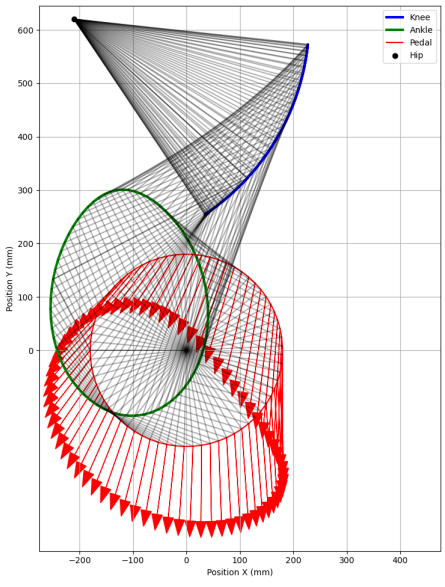


Figure 5. Pedal force generated by a full activation of the gluteus maximus in all pedal positions.

In Fig. 5, we can see the course done by the knee in blue, showing how narrow is the use of the gluteus maximus in this pedaling configuration. The green circular line represents the position of the ankle in the cycle. The red circle represents the pedal course and the vector's are pointing in the direction of the force done by the foot on the pedal. Analyzing the force directions, we can see that only a portion of them will move the bicycle forward, and even less, are in a perpendicular direction with respect to the crank arm. This indicates that, even

with an increase in force magnitude, when the pedal is close to the bottom position, the gluteus maximus does not efficiently generate torque at the crankshaft.

Graphing the torque along a crank rotation, Fig. 6, we can see that the maximum torque is reached at an angle just before zero degrees. This angle corresponds to the 3 o'clock position on the bicycle of Fig. 1 and Fig. 5. The green area corresponds to the positive torque that will generate a forward movement and the approximate range of crank position where it happens is from $-68°$ to $+97°$.

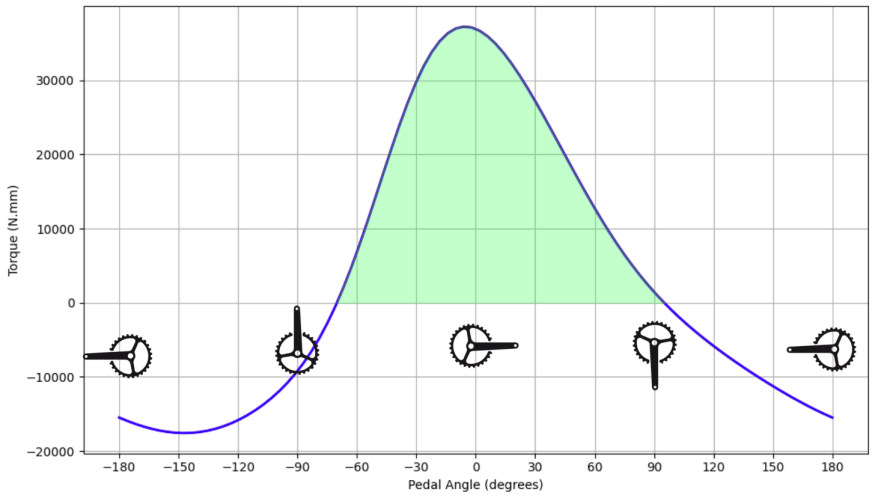


Figure 6. Crank torque generated by the gluteus maximus along a crank rotation.

Looking at the hip torque generated by the gluteus maximus in Fig. 7, we can notice that the maximum crank torque is not in phase with the peak hip torque saw in Fig. 6. The Zero Crank Torque arrows indicate the positions where isometric muscle contraction occurs, resulting in low torque generation in the crankcase. This indicates an opportunity to reconfigure the cyclist's position, but it also explains why people stand up when they need to increase pedal force.

At this point, we have shown a method for modeling a leg muscle and how to use it to predict force and torque during the pedaling cycle. Now the study can continue modeling all leg muscles relevant to the pedaling cycle, and compare it to actual measurements from bikers to see if it can correctly predict the forces and moments, or if it need some kind of calibration to do so.

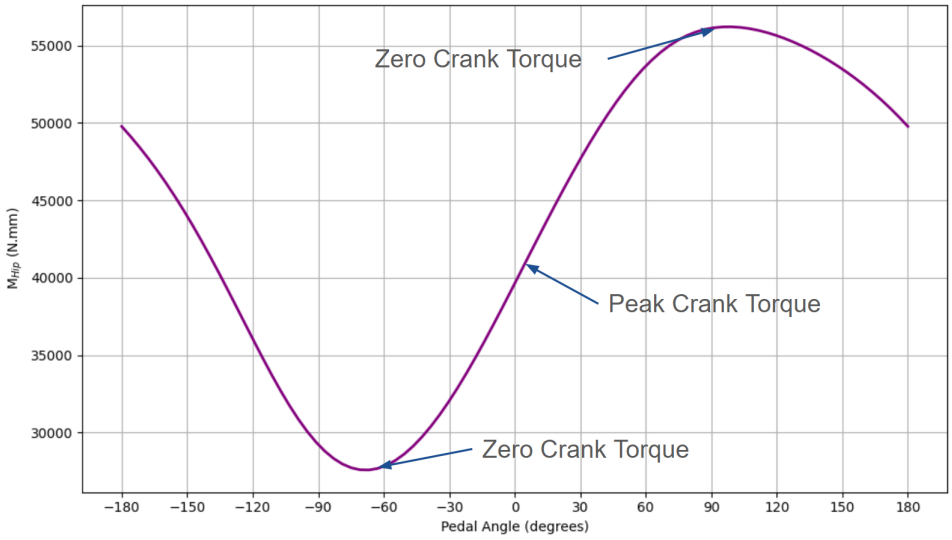


Figure 7. Hip torque generated by the gluteus maximus along a crank rotation.

4 Conclusions

This study presents a biomechanical modeling approach that quantifies the contribution of the gluteus maximus to pedal torque during cycling. The main findings indicate that the gluteus maximus generates significant torque during a limited portion of the crank cycle. The cyclist's seated position reduces the gluteus efficiency, as the moment arm shortens with hip flexion, limiting torque transmission. The current seated posture commonly adopted by cyclists may reduce the efficiency of gluteus maximus force transmission due to suboptimal joint angles and moment arms. Even under full activation, much of the muscle effort does not effectively translate into crank torque, due to the poor mechanical advantage in most positions.

The developed model confirms that muscle force and torque production depend heavily on anatomical constraints and nonlinear muscle properties, especially muscle length and moment arm variation. Being parametric and allowing for fast recalculations, it is capable of adapting to different anthropometries and is useful for optimizing frame geometry or drivetrain configurations.

The framework developed allows for subject-specific simulations and can serve as a foundation for optimizing bicycle drivetrain components, such as noncircular chainrings, to improve uphill cycling performance.

Future work will include the integration of additional muscles and experimental validation to further enhance model accuracy and practical applications. From a computational engineering perspective, this model creates a foundation for future numerical optimization studies. It can be used to evaluate the effect of drivetrain geometries, including noncircular chainrings, or to guide the design of cyclist-specific components. The modular code structure and linear system formulation also make it suitable for integration with optimization algorithms or multibody dynamics platforms.

Acknowledgements. The authors thanks the financial support of CAPES (Coordenação de Aperfeiçoamento de Pessoal de Nível Superior), Brazil, under grant number 88887.005477/2024-00.

Authorship statement. The authors hereby confirm that they are the sole liable persons responsible for the authorship of this work, and that all material that has been herein included as part of the present paper is either the property (and authorship) of the authors, or has the permission of the owners to be included here.

References

[1] J. Juhl. Non-circular chainring optimization for handcycling. *Journal of Loremipsum*, vol. 01, n. 1, pp. 1–8. Department of Health Science and Technology, Aalborg University, 2013.

[2] R. Redfield and M. L. Hull. Prediction of pedal forces in bicycling using optimization methods. *Journal of Biomechanics*, vol. 19, n. 7, pp. 523–540, 1986.

[3] B. Fonda and N. Šarabon. Biomechanics and energetics of uphill cycling: A review. *Kinesiology*, vol. 44, n. 1, pp. 5–17, 2012.

[4] M. L. Hull and M. Jorge. A method for biomechanical analysis of bicycle pedalling. *Journal of Biomechanics*, vol. 18, n. 9, pp. 631–644, 1985.

[5] R. F. Chandler, C. E. Clauser, J. T. McConville, H. M. Reynolds, and J. W. Young. Investigation of inertial properties of the human body. Technical Report AMRL-TR-74-137, Aerospace Medical Research Laboratory, Air Force Systems Command, Wright-Patterson Air Force Base, Wright-Patterson AFB, OH. Prepared for the U.S. Department of Transportation, National Highway Traffic Safety Administration, under Contract No. DOT-HS-017-2-315-1A, 1975.

[6] S. R. Ward, C. M. Eng, L. H. Smallwood, and R. L. Lieber. Are current measurements of lower extremity muscle architecture accurate? *Clinical Orthopaedics and Related Research*, vol. 467, n. 4, pp. 1074–1082, 2009.

[7] L. S. Persad, M. Malekzadeh, A. M. Maga, C. M. Eng, and S. R. Ward. Specific tension of human muscle in vivo: a systematic review. *Journal of Applied Physiology (Bethesda, Md. : 1985)*, vol. 137, n. 4, pp. 945–962, 2024.

[8] D. G. Thelen. Adjustment of muscle mechanics model parameters to simulate dynamic contractions in older adults. *Journal of Biomechanical Engineering*, vol. 125, n. 1, pp. 70–77, 2003.

[9] W. M. Murray, T. S. Buchanan, and S. L. Delp. The isometric functional capacity of muscles that cross the elbow. *Journal of Biomechanics*, vol. 33, n. 8, pp. 943–952, 2000.

[10] D. E. Rassier, B. R. MacIntosh, and W. Herzog. Length dependence of active force production in skeletal muscle. *Journal of Applied Physiology*, vol. 86, n. 5, pp. 1445–1457, 1999.

[11] E. M. Arnold, S. R. Ward, R. L. Lieber, and S. L. Delp. Accuracy of muscle moment arms estimated from mri-based musculoskeletal models of the lower extremity. *Computer Aided Surgery*, vol. 5, n. 2, pp. 108–119,

2000.
[12] L. Modenese and J. Kohout. Automated generation of three-dimensional complex muscle geometries for use in personalised musculoskeletal models. *Annals of Biomedical Engineering*, vol. 48, n. 6, pp. 1793–1804, 2020.
[13] Z. Chen and D. W. Franklin. Muscle moment arm–joint angle relations in the hip, knee, and ankle: A visualization of datasets. *bioRxiv*. Preprint. Available under CC-BY 4.0 license, 2024.
[14] G. Németh and H. Ohlsén. In vivo moment arm lengths for hip extensor muscles at different angles of hip flexion. *Journal of Biomechanics*, vol. 18, n. 2, pp. 129–138, 1985.
[15] C. M. Eng, A. S. Arnold, D. E. Lieberman, and A. A. Biewener. The capacity of the human iliotibial band to store elastic energy during running. *Journal of Biomechanics*, vol. 48, n. 12, pp. 3341–3348, 2015.